Success Probability in Wirelessly Powered Networks with Energy Correlation

Na Deng* and Martin Haenggi†
*School of Information & Communication Engineering, Dalian University of Technology, Dalian, 116024, China
†Dept. of Electrical Engineering, University of Notre Dame, Notre Dame, IN, 46556, USA
Email:*dengna@dlut.edu.cn, †mhaenggi@nd.edu

***Abstract*—In the analysis of large-scale wirelessly powered networks, the energy correlation is often ignored for analytical tractability. Accounting for the energy correlation, this paper introduces and promotes the Poisson disk process (PDP) as a model for the active RF-powered nodes that succeed in harvesting energy. To show that the model leads to tractable results in several cases of interest, we derive the density and second moment density of the PDP and find the key property that the PDP can be fully characterized by its first- and second-order statistics. Tight bounds for its probability generating functional (PGFL) are also provided. To show that the model is relevant for wirelessly powered networks that exhibit positive energy correlation, we fit the PDP to a given energized point process incorporating practical energy harvesting factors and derive the information transmission success probability. It turns out that the resulting PDP can closely model the distribution of actual energized RF-powered nodes in terms of the success probability and other statistics while preserving analytical tractability.**

I. Introduction

As a powerful tool for the performance analysis of wireless networks, stochastic geometry has naturally been the preferred choice for modeling and analyzing wirelessly powered networks due to its realism in capturing the irregularity of node locations [1]. The authors in [2] investigated the tradeoffs between transmit power and density of mobile devices and wireless power beacons which are modeled as two independent homogeneous Poisson point processes (PPPs). As an extension, the work of [3] studied wireless energy harvesting in an uplink K-tier cellular network, where the locations of the users and base stations (BSs) were modeled using independent PPPs. Analytical results on wireless energy harvesting were also obtained for relay [4], cognitive [5], device-to-device [6], and millimeter-wave [7] networks in a stochastic geometry-based framework.

Although many efforts have been made, the research in this direction mostly focuses on the setting where the active communication nodes simply form an independent thinning of the RF-powered nodes, which are independent of the RF power sources. As a result, the network topology in the energy transfer phase is independent of that in the communication phase. This clearly deviates from reality since the energy transfer performance has a fundamental impact on the topology of the energized RF-powered nodes (i.e., the active communication nodes) and hence the communication performance. The connection between the energy and information transfer fundamentally lies in the spatial correlation of the amount of energy that can be harvested by RF-powered nodes, namely the energy correlation. In order to capture the energy correlation in wirelessly powered networks, a new point process, named *energized point process* (EPP), has recently been proposed to model the energized RF-powered nodes [8]. It is a general model that can be concretized for any given energy harvesting model. However, the drawback is that an exact characterization of the system performance indicators, such as the success probability and area spectral efficiency, becomes quite challenging. The only approach so far is to use a homogeneous PPP or a Poisson cluster process (PCP) to approximate the EPP [8], which usually leads to either inaccurate or complex-form analytical results. To our best knowledge, tractable models that accurately model the wirelessly powered networks with energy correlation are still unavailable, an issue that needs to be resolved urgently.

In this paper, we focus on the Poisson disk process (PDP) where disks are created around nodes (namely the RF transmitters) modeled by a homogeneous PPP and only the RF-powered nodes located within disks are retained. The PDP is a simple type of EPP where an RF-powered node succeeds in harvesting enough energy if and only if there is at least one RF transmitter within a given distance. As such, it achieves a good tradeoff between modeling accuracy and tractability.

II. Mathematical Preliminaries

Here we give a brief overview of some terminology and mathematical tools from stochastic geometry. Readers are referred to [1, 9, 10] for further details.

Definition 1 (Germ-grain model [1, Def. 13.1]). *Let $\Phi = \{x_1, x_2, \ldots\}$ be a point process on $\mathbb{R}^2$, the germs, and $(S_1, S_2, \ldots)$ a collection of random non-empty sets, the grains. Then the union $\Xi = \bigcup_{i\in\mathbb{N}} x_i + S_i$ is a germ-grain model.*

Definition 2 (Boolean model [1, Def. 13.4]). *A Boolean model is a germ-grain model where the germ point process is a uniform PPP and the grains S_i are i.i.d.*

Definition 3 (Boolean Cox process on disks [9, Sec. 2.1]). *Let $\Xi = \bigcup_{i\in\mathbb{N}} b(y_i, R)$ be a Boolean germ-grain model where $\{y_1, y_2, \ldots\}$ is a stationary Poisson point process with intensity $\beta > 0$ and $b(y_i, R)$ denotes a disk centered at y_i with*

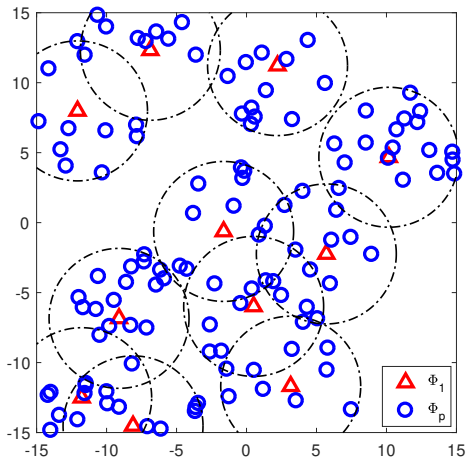

Fig. 1. A realization of the PDP with $\beta = 0.01$, $\lambda_{\rm I} = 0.2$, and $R = 5$.

radius R. Then, let $\Phi = \{x_1, x_2, \ldots\}$ be a Cox process with random driving measure Λ induced by Ξ as

$$\Lambda(\mathrm{d}x) = \begin{cases} \lambda_{\rm I}\mathrm{d}x & \text{if } x \in \Xi \\ \lambda_{\rm II}\mathrm{d}x & \text{if } x \notin \Xi \end{cases} \tag{1}$$

where $0 \le \lambda_{\rm I}, \lambda_{\rm II} < \infty$ and $\max\{\lambda_{\rm I}, \lambda_{\rm II}\} > 0$. This Cox process is called Boolean Cox process on disks.

Note that when $\lambda_{\rm I} = 0$, it reduces to the Swiss cheese model (also called Poisson hole process [10, 11]); and when $\lambda_{\rm II} = 0$, it reduces to the inner-city model [1].

III. The Poisson Disk Process

A. Definition

Definition 4 (Poisson disk process, PDP). *The Poisson disk process is a Boolean Cox process on disks with $\lambda_{\rm II} = 0$.*

Fig. 1 shows an example realization of the PDP. From the definition, the PDP $\Phi_{\rm p}$ can be described by a Boolean model on disks $\Xi = \bigcup_{y\in\Phi_1} b(y, R)$ with two PPPs Φ_1 and Φ_2 of densities β and $\lambda_{\rm I}$, respectively. Hence we have $\Phi_{\rm p} = \Phi_2 \cap \Xi$. The PDP is a dependent thinning of Φ_2 and can be viewed as a Cox process with intensity field $\kappa_{\rm p}(x) = \lambda_{\rm I}\mathbf{1}\big(\Phi_1\big(b(x,R)\big) > 0\big)$, where $\mathbf{1}(\cdot)$ denotes the indicator function and $\Phi_1\big(b(x,R)\big)$ is the number of points in Φ_1 located in $b(x,R)$.

B. Basic Properties

Since $\Phi_{\rm p}$ is motion-invariant, its density is a constant and its second moment density $\rho^{(2)}(x,y) = \rho^{(2)}_{\rm mi}(u)$ depends only on the distance $u = \|x - y\|$. For the density of the PDP, we have $\lambda_{\rm p} = \lambda_{\rm I} P_{\rm p}(R)$, where $P_{\rm p}(R)$ is the retaining probability of a point at the origin [9], given by

$$P_{\rm p}(R) = 1 - \exp(-\beta\pi R^2). \tag{2}$$

The second moment density is a key statistic that describes the pairwise correlation of a point process. For the PPP, $\rho^{(2)}(x,y) = \lambda^2$, because points are independent. If $\rho^{(2)}(x,y) > \lambda^2$, points at distance $\|x-y\|$ exhibit clustering, and if $\rho^{(2)}(x,y) < \lambda^2$, points exhibit repulsion. In the following lemma, we give a closed-form expression for the second moment density of the PDP $\rho^{(2)}_{\rm mi}(u)$.

Lemma 1. *The second moment density $\rho^{(2)}_{\rm mi}(u)$ of the PDP is*

$$\rho^{(2)}_{\rm mi}(u) = \lambda_{\rm I}^2\Big(1 - 2e^{-\beta\pi R^2} + e^{-\beta\left(2\pi R^2 - A(R,u)\right)}\Big), \tag{3}$$

where

$$A(R,u) = \begin{cases} 2R^2 \arccos\left(\frac{u}{2R}\right) - u\sqrt{R^2 - \frac{u^2}{4}} & \text{if } u \le 2R \\ 0 & \text{otherwise} \end{cases} \tag{4}$$

is the intersection area of two disks with radius R at distance u.

Proof: See Appendix A

According to [1, Def. 6.6], the pair correlation function is given by

$$\begin{aligned} g_{\rm p}(u) &\triangleq \frac{\rho^{(2)}_{\rm mi}(u)}{\lambda_{\rm p}^2} \\ &= 1 + \frac{e^{-2\beta\pi R^2}\left(e^{\beta A(R,u)} - 1\right)}{(1 - e^{-\beta\pi R^2})^2}. \end{aligned} \tag{5}$$

As expected from the clustered nature of the PDP, $g_{\rm p}(u) \ge 1$ for all $u \ge 0$. Given the density $\lambda_{\rm p}$ and the pair correlation function $g_{\rm p}(u)$, we obtain for the PDP that

$$R = \frac{1}{2}\min_{u>0}\{u\colon g_{\rm p}(u) = 1\}, \tag{6}$$

$$\beta = \frac{1}{\pi R^2}\log\frac{g_{\rm p}(0)}{g_{\rm p}(0) - 1}, \tag{7}$$

$$\lambda_{\rm I} = \lambda_{\rm p}/g_{\rm p}(0). \tag{8}$$

Thus, the PDP is fully characterized by its first-order statistic $\lambda_{\rm p}$ and its second-order statistic $g_{\rm p}(u)$ (or $\rho^{(2)}(u)$)[1]. This implies that a suitable PDP can be used to generate point distributions with any given intensity and pair correlation function that satisfy certain constraints.

C. Probability generating functional

The PGFL is a key tool in a point process theory, which has many applications in wireless networks. Most notably, it can be used to evaluate the Laplace transform of the sum of all the interfering signal powers emitted from a PDP field of interferers. In this subsection, we consider the PGFL conditioning on that there is a point of the process $\Phi_{\rm p}$ at the origin but without including the point. Denoting by $\mathbb{E}^{!o}(\cdot)$ the expectation with respect to the reduced Palm measure [1, Def. 8.4.1], the conditional PGFL is defined as

$$\mathcal{G}^{!}[v] \triangleq \mathbb{E}^{!o}\Big(\prod_{x\in\Phi_{\rm p}} v(x)\Big), \tag{9}$$

where v is a function: $\mathbb{R}^2 \mapsto [0,1]$ such that $1 - v$ has bounded support. For notational convenience, we define

[1]The Matérn cluster process also has this property but not the Thomas cluster process [1].

$V(R,y) \triangleq \int_{b(y,R)}[1-v(x)]\mathrm{d}x$, $b^c(o,t) \triangleq \mathbb{R}^2 \setminus b(o,t)$ and $y_0 \triangleq \arg\min\{y \in \Phi_1 \colon \|y\|\}$. Next, we derive bounds and approximation on the conditional PGFL.

Theorem 1 (**Bounds on the conditional PGFL of the PDP**). *Let*

$$\hat{\mathcal{G}}^!_{\mathrm{p}}[v] \triangleq \frac{1}{P_{\mathrm{p}}(R)} \int_{b(o,R)} \beta e^{-\beta\pi\|y\|^2-\lambda_{\mathrm{I}}V(R,y)}\mathrm{d}y, \tag{10}$$

$$\check{\mathcal{G}}^!_{\mathrm{p}}[v] \triangleq \frac{1}{P_{\mathrm{p}}(R)} \int_{b(o,R)} \beta e^{-\beta\pi\|x\|^2-\lambda_{\mathrm{I}}V(R,x)} \times \exp\Big(-\beta\int_{b^c(o,\|x\|)} 1-e^{-\lambda_{\mathrm{I}}V(R,y)}\mathrm{d}y\Big)\mathrm{d}x. \tag{11}$$

The conditional PGFL of the PDP is bounded by $\check{\mathcal{G}}^!_{\mathrm{p}}[v] < \mathcal{G}^!_{\mathrm{p}}[v] < \hat{\mathcal{G}}^!_{\mathrm{p}}[v]$.

Proof: See Appendix B.

Since $b^c(o,R) \subset b^c(o,\|x\|)$ if $x \in b(o,R)$, the lower bound $\check{\mathcal{G}}^!_{\mathrm{p}}[v]$ with three nested integrals can be used to obtain an approximation in a simpler form (two nested integrals) as

$$\check{\mathcal{G}}^!_{\mathrm{p}}[v] \approx \frac{1}{P_{\mathrm{p}}(R)} \exp\Big(-\beta\int_{b^c(o,R)} 1-e^{-\lambda_{\mathrm{I}}V(R,y)}\mathrm{d}y\Big) \times \int_{b(o,R)} \beta e^{-\beta\pi\|y\|^2-\lambda_{\mathrm{I}}V(R,y)}\mathrm{d}y. \tag{12}$$

Remark 1: To maintain tractability, the overlaps of the disks in the Boolean model are not considered in deriving the lower bounds. Thus, the tightness of the lower bounds greatly depends on the number of disks that cause a point to be retained, which follows a Poisson distribution with mean $\beta\pi R^2$ [1, Thm. 13.5]. Denoting by P_{c} the probability that the typical point is covered by less than two disks, we have $P_{\mathrm{c}} = e^{-\beta\pi R^2}(1+\beta\pi R^2)$. Then, when $P_{\mathrm{c}} \to 1$, i.e., $\beta\pi R^2 \to 0$, the lower bounds get remarkably tight without losing analytical tractability.

Remark 2: As for the upper bounds, since only the closest disk to the origin in the Boolean model is considered, thereby neglecting the effect of the distant points in the PDP, the tightness of the uppers bounds is mainly determined by the monotonicity of $v(x)$ with $\|x\|$ and the number of points of Φ_2 in the closest disk. For instance, when $v(x)$ is monotonically decreasing with $\|x\|$, e.g., when using it to represent path loss, the upper bounds are also remarkably tight.

IV. System Model

In this section, we apply the PDP to a wirelessly powered network. As discussed above, there is spatial correlation among the amount of harvested energy by RF-powered nodes. We first formally define the EPP and then establish the key relationship between the PDP and the EPP.

A. Energized point process

Definition 5 (**Energized point process** [8]). *Let* Φ_{f} *and* Φ_{d} *be two point processes of RF transmitters and RF-powered nodes, respectively. Then the energized point process* Φ_{e} *is defined as a dependent thinning of* Φ_{d} *as*

$$\Phi_{\mathrm{e}} \triangleq \{x \in \Phi_{\mathrm{d}} \colon E(x,\Phi_{\mathrm{f}}) = 1\}, \tag{13}$$

where $E(x,\Phi_{\mathrm{f}}) \in \{0,1\}$ *is the energy indicator function describing whether enough energy can be harvested from* Φ_{f} *at location* x.

In this paper, the two point processes Φ_{f} and Φ_{d} are assumed to be two independent homogeneous PPPs with densities λ_{f} and λ_{d}, respectively. Then the energy indication function is

$$E(x,\Phi_{\mathrm{f}}) = \mathbf{1}(\varepsilon(x,\Phi_{\mathrm{f}}) > \xi), \tag{14}$$

where $\varepsilon(x,\Phi_{\mathrm{f}})$ denotes the energy harvested from Φ_{f} at location x and ξ is the energy threshold.

It is assumed that the RF signals merely experience large-scale path loss, and a linear energy harvesting model is adopted. Hence, the harvested energy at x is the aggregate received signal strength from all the RF transmitters in Φ_{f}, which is given by

$$\varepsilon(x,\Phi_{\mathrm{f}}) = \sum_{y\in\Phi_{\mathrm{f}}} \ell(y-x), \tag{15}$$

where $\ell(x) \triangleq \|x\|^{-\alpha}$ is the path loss function with exponent α for the energy transfer link.

B. PDP Model for EPP

Compare Definitions 4 and 5, and let Φ_1 be Φ_{f}, β be λ_{f}, Φ_2 be Φ_{d}, and λ_{I} be λ_{d}. It is easily seen that the PDP behaves like an EPP but has a simpler structure than the EPP. Thus, it is intuitive to use the PDP as a tractable model for the active RF-powered nodes, by establishing a relationship between the PDP model and a given EPP that incorporates practical energy harvesting factors. The basic idea is to determine R by setting $\mathbb{P}\big(\Phi_{\mathrm{f}}(b(x,R)) > 0)\big) = \mathbb{P}\big(\varepsilon(x,\Phi_{\mathrm{f}}) > \xi\big)$ such that $\lambda_{\mathrm{p}} = \lambda_{\mathrm{e}}$. Due to the motion-invariance of Φ_{p}, $\mathbb{P}\big(\varepsilon(x,\Phi_{\mathrm{f}}) > \xi\big) = \mathbb{P}\big(\varepsilon(o,\Phi_{\mathrm{f}}) > \xi\big) \triangleq P_{\mathrm{e}}$ is the energy harvesting success probability of the RF-powered node at the origin. Let $\varphi(w) \triangleq \mathbb{E}(e^{jw\varepsilon(o,\Phi_{\mathrm{f}})})$ be the characteristic function of the harvested energy at the origin. According to [1, Sec. 5.15], the characteristic function for $\alpha > 2$ is expressed as

$$\varphi(w) = \exp\big(-\lambda_{\mathrm{f}}\pi\Gamma(1-\delta)w^{\delta}e^{-j\pi\delta/2}\big), \quad w \geq 0, \tag{16}$$

where $j = \sqrt{-1}$ and $\delta = 2/\alpha$. Using the Gil-Pelaez theorem [12], we have

$$P_{\mathrm{e}} = \frac{1}{2} + \frac{1}{\pi}\int_0^{\infty} \frac{\Im\big(e^{-jw\xi}\varphi(w)\big)}{w}\mathrm{d}w. \tag{17}$$

Then, according to (2) and $\mathbb{P}\big(\Phi_{\mathrm{f}}(b(o,R)) > 0)\big) = P_{\mathrm{e}}$, we have

$$R = \sqrt{\frac{1}{\pi\lambda_{\mathrm{f}}}\ln\frac{1}{1-P_{\mathrm{e}}}}. \tag{18}$$

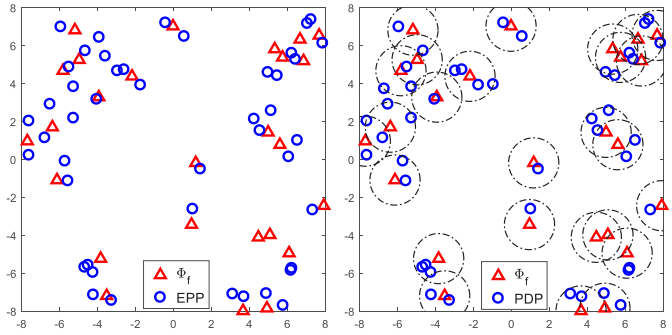

Fig. 2. Comparison of the EPP (left) and the fitted PDP (right) with $R = 1.32$, where $\lambda_f = 0.1$, $\lambda_d = 1$, $\xi = 0.5$, and $\alpha = 4$.

1) Special Case: When $\alpha = 4$, we have

$$\varphi(w) = \exp\big(-\lambda_f \pi^{3/2}\sqrt{w}e^{-j\pi/4}\big), \quad w \geq 0, \tag{19}$$

and in this case the energy harvesting success probability admits a closed-form expression, given by

$$P_e = 1 - \frac{1}{\sqrt{\pi}}\Gamma\Big(\frac{1}{2}, \frac{\pi^3\lambda_f^2}{4\xi}\Big). \tag{20}$$

2) Special Case: When $\alpha \to \infty$, we have $\ell(x) \to 0$ for $\|x\| > 1$ and $\ell(x) \to \infty$ for $\|x\| < 1$. For the EPP in this case, only those points with a distance to the RF transmitters smaller than 1 can be energized. As a result, the EPP converges to the PDP with $R = 1$. This observation further justifies the use of the PDP to characterize the EPP.

Fig. 2 shows a comparison between the realizations of the EPP and the fitted PDP under the same realization of Φ_f and Φ_d. It is observed that the points retained in the EPP are almost the same as those retained in the PDP, which demonstrates the good match between the two point processes.

C. Communication Model

Each energized RF-powered node is assumed to have a dedicated receiver at distance d in a random orientation. Hence, the energized RF-powered nodes and their receivers form a Cox (PDP) bipolar network. The transmit power of RF-powered nodes is assumed to be one. We further assume that all power fading coefficients are i.i.d. exponential (Rayleigh fading) with a mean of one. Due to the stationarity of the PDP, we condition on that the typical transmitter (active RF-powered node) is located at the origin, with the corresponding typical receiver at $z = (d, 0)$. Letting $\Phi_p^o \triangleq (\Phi_p \mid o \in \Phi_p)$ and $\Phi_p^{!o} \triangleq \Phi_p^o \setminus \{o\}$, the received SIR of the typical receiver is given by

$$\mathrm{SIR} = \frac{\ell(z)h_{oz}}{I^!(z)}, \tag{21}$$

where $I^!(z) \triangleq \sum_{x\in\Phi_p^{!o}} \ell(x-z)h_{xz}$ is the interference.

V. Analysis of Transmission Success Probability

In this section, we provide the information transmission success probability analysis of a wirelessly powered network, where the locations of the transmitters in the communication phase (i.e., the energized RF-powered nodes) are modeled by a PDP. The success probability is defined as $P(\theta) \triangleq \mathbb{P}(\mathrm{SIR} > \theta)$ and can be derived through the Laplace transform of the interference, where θ is the SIR threshold.

Letting $\mathcal{L}_{I^!}(s)$ be the conditional Laplace transform of $I^!$, we have

$$\mathcal{L}_{I^!}(s) = \mathbb{E}^{!o}\Big[\prod_{x\in\Phi_p} \frac{1}{1+s\ell(x-z)}\Big] = \mathcal{G}^!\Big[\frac{1}{1+s\ell(x-z)}\Big]. \tag{22}$$

In the bipolar communication model, since the distance d between a transmitter-receiver pair is usually set relatively small (i.e., $d \ll \lambda_p^{-1/2}$), we approximate $I^!(z)$ with $I^!(o)$, resulting in $\mathcal{L}_{I^!}(s) \approx \mathcal{G}^![\frac{1}{1+s\ell(x)}]$. Then the following analytical results concerning $\mathcal{L}_{I^!}(s)$ with small d can be significantly simplified. Let $\check{\mathcal{L}}_{I^!}(s)$ and $\hat{\mathcal{L}}_{I^!}(s)$ be a lower and upper bound on $\mathcal{L}_{I^!}(s)$, respectively. Using the polar coordinates, we have

$$\check{\mathcal{L}}_{I^!}(s) \overset{(b)}{\approx} \frac{2\pi\lambda_f \int_0^R e^{-\lambda_f\pi v^2 - \lambda_d\gamma(v,R,s)} v\mathrm{d}v}{P_p(R)} \times e^{-2\pi\lambda_f\int_R^\infty \left(1-e^{-\lambda_d\gamma(v,R,s)}\right)v\mathrm{d}v}, \tag{23}$$

$$\hat{\mathcal{L}}_{I^!}(s) = \frac{2\pi\lambda_f}{P_p(R)}\int_0^R e^{-\lambda_f\pi v^2 - \lambda_d\gamma(v,R,s)} v\mathrm{d}v, \tag{24}$$

where step (b) is obtained using the simplified approximation in (12). If $v \leq R$, we have

$$\gamma(v,R,s) = 2\pi\int_0^{R-v} \frac{r\mathrm{d}r}{1+s^{-1}r^\alpha} + 2\int_{R-v}^{R+v} \frac{\arccos\left(\frac{v^2+r^2-R^2}{2vr}\right)r\mathrm{d}r}{1+s^{-1}r^\alpha}, \tag{25}$$

otherwise,

$$\gamma(v,R,s) = 2\int_{v-R}^{R+v} \frac{\arccos\left(\frac{v^2+r^2-R^2}{2vr}\right)r\mathrm{d}r}{1+s^{-1}r^\alpha}. \tag{26}$$

It is worth noting that the success probability necessarily tends to zero for $\theta \to \infty$ while its upper bound $\hat{\mathcal{L}}_{I^!}(\theta d^\alpha)$ tends to $e^{-\lambda_d\pi R^2}$. This indicates that the upper bound on the success probability deviates more from the exact result when θ gets large. This is mainly due to the fact that the upper bound of the PGFL $\hat{\mathcal{G}}^![v]$ is obtained by merely considering the points in $\Phi_2 \cap b(y_0, R)$ with $y_0 \in \Phi_1$ the nearest point to the origin, thereby neglecting the contribution from the more distant points in Φ_p. To solve this problem, we further approximate the spatial distribution of the points in $\Phi_2 \backslash b(y_0, R)$ with a PPP with density λ_p, which results in an accurate approximation to the Laplace transform of the interference, given in the following corollary.

Corollary 1. *Let* $\tilde{\gamma}(v,R,s) = 2\pi\int_{R+v}^\infty \frac{r}{1+s^{-1}r^\alpha}\mathrm{d}r$ *and*

$$\tilde{\mathcal{L}}_{I^!}(s) \triangleq \frac{2\pi\lambda_f}{P_p(R)}\int_0^R e^{-\lambda_f\pi v^2 - \lambda_d\gamma(v,R,s) - \lambda_p\tilde{\gamma}(v,R,s)} v\mathrm{d}v, \tag{27}$$

and the Laplace transform of the interference is approximated as $\mathcal{L}_{I^!}(s) \approx \tilde{\mathcal{L}}_{I^!}(s)$.

Proof: See Appendix C.

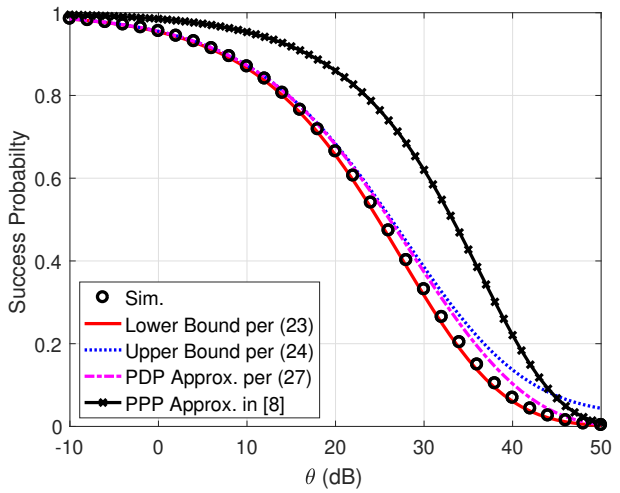

Fig. 3. The validation of the analytical results derived from the PDP.

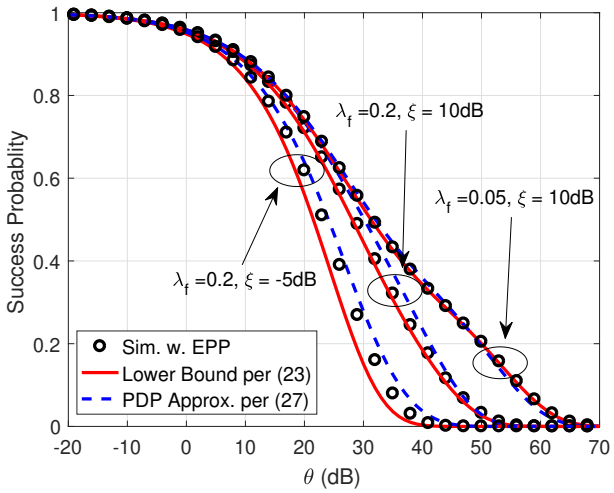

Fig. 4. The success probability of the PDP-based network.

VI. Numerical Results

In this section, we provide the numerical results concerning the success probability in PDP-modeled wirelessly powered network with energy correlation. The default values of the main parameters are $\beta = \lambda_{\rm f} = 0.1$, $\lambda_{\rm I} = \lambda_{\rm d} = 1$, $\alpha = 4$, $\xi = 1$ and $d = 0.1$ where applicable.

Fig. 3 compares the transmission success probability in the communication phase using different approaches, where the simulation result is based on a given EPP incorporating practical energy harvesting factors. We observe that both the proposed bounds and the approximation by the PDP are quite close to the simulation results, demonstrating the effectiveness and rationality of using the PDP to characterize the EPP. Furthermore, it can be seen that the PPP-based results always deviate from the simulations obviously despite of its simplicity.

Fig. 4 compares the EPP-based simulations and the PDP-based analytical results for different RF transmitter densities and energy thresholds. It is observed that the PDP-based approximation matches with the actual result extremely well for different parameter setups since it incorporates both strong interferers nearby and the weak ones far away. The lower bound is tight for certain parameter settings, e.g., for a small density of RF transmitters (sparse deployment) or a large energy threshold (strong clustering behavior). The reason is that the overlaps among different disks are ignored in the PDP model, and the larger $\lambda_{\rm f}$ or the smaller ξ (leading to a larger R), the more likely the overlaps occur.

VII. Conclusions

Since the energy correlation establishes a dependence between energy and information transfer, it plays an important role in the communication phase. Although some prior work has addressed the energy correlation issue, an exact characterization of the communication performance is still unavailable. Our work is the first to propose a tractable yet accurate model, named PDP, for the energized RF-powered nodes and focus on the accurate performance characterization of a wirelessly powered network with energy correlation.

We first investigated the basic properties of the PDP and used it as a model for characterizing a given point set of EPP considering practical energy harvesting factors. Interestingly, the PDP can be viewed as a kind of EPP but with a simpler structure, which is fully characterized by its first- and second-order statistics. Secondly, we provided tight bounds as well as accurate approximation for its PGFL and its application to the analysis of the information transmission success probability. We show that, remarkably, the PDP is superior to the PPP in balancing the accurate modeling and analytical tractability.

Acknowledgment

This work has been supported by National Natural Science Foundation of China (61701071), the China Postdoctoral Science Foundation (2017M621129 and 2019T120204), the Fundamental Research Funds for the Central Universities (DUT19RC(4)014).

Appendix A
Proof of Lemma 1

Proof: According to the definition of Ripley's K function [1, Def. 6.8], we have

$$\lambda_{\rm p} K(r) = \frac{2\pi}{\lambda_{\rm p}} \int_0^r \rho_{\rm mi}^{(2)}(u) u {\rm d}u, \tag{28}$$

where $\lambda_{\rm p} K(r)$ is the mean number of points $y \in \Phi_{\rm p}$ that satisfy $0 \le \|y - x\| \le r$ given that $x \in \Phi_{\rm p}$. Hence we have

$$\begin{aligned}
&\lambda_{\rm p} K(r) \\
=&\mathbb{E}^{!o}[\Phi_{\rm p}(b(o,r))] \\
=&\mathbb{E}\Big[\sum_{y\in\Phi_2} \mathbf{1}\big(\|y\| < r \cap \Phi_1\big(b(y,R)\big) > 0\big) \,|\, \Phi_1\big(b(o,R)\big) > 0\Big] \\
\overset{(a)}{=}&\lambda_{\rm I} \int_{b(o,r)} \mathbb{P}\Big(\Phi_1\big(b(y,R)\big) > 0 \,|\, \Phi_1\big(b(o,R)\big) > 0\Big) {\rm d}y
\end{aligned}$$

$$=\frac{\lambda_{\rm I}^2}{\lambda_{\rm p}}\int_{b(o,r)}\mathbb{P}\Big(\Phi_1\big(b(y,R)\big)>0,\Phi_1\big(b(o,R)\big)>0\Big)\mathrm{d}y, \quad (29)$$

where step (a) uses Campbell's theorem. Letting $u \triangleq \|y\|$, $V_u(R) \triangleq b(o,R)\cap b(y,R)$ and $b^c(y,R) \triangleq b(y,R)\setminus V_u(R)$, the event $\{\Phi_1\big(b(y,R)\big)>0,\Phi_1\big(b(o,R)\big)>0\}$ is partitioned into two events: one is $\{\Phi_1\big(V_u(R)\big)>0\}$; the other is $\{\Phi_1\big(b^c(o,R)\big)>0,\Phi_1\big(b^c(y,R)\big)>0\}$ conditioning on $\{\Phi_1\big(V_u(R)\big)=0\}$. According to the total probability law and polar coordinates, we have

$$\lambda_{\rm p}K(r)=\frac{2\pi\lambda_{\rm I}^2}{\lambda_{\rm p}}\int_0^r\Big(1-2e^{-\beta\pi R^2}+e^{-\beta(2\pi R^2-A(R,u))}\Big)u\mathrm{d}u. \quad (30)$$

Comparing (29) and (30), the final result is obtained. ∎

Appendix B
Proof of Theorem 1

Proof: According to the Boolean model, we have

$$\begin{aligned}
\mathcal{G}^![v]&=\mathbb{E}^{!o}\Big(\prod_{x\in\Phi_{\rm p}}v(x)\Big)\\
&=\mathbb{E}^{!o}\Big[\prod_{x\in\Phi_2\cap\Xi}v(x)\mid\Phi_1(b(o,R))>0\Big]\\
&>\mathbb{E}^{!o}\Big(\prod_{y\in\Phi_1}\prod_{x\in\Phi_2\cap b(y,R)\setminus\{o\}}v(x)\mid\Phi_1(b(o,R))>0\Big)\\
&=\mathbb{E}_{\Phi_1}\Big[\prod_{y\in\Phi_1}\mathbb{E}^{!o}_{\Phi_2}\Big(\prod_{x\in\Phi_2\cap b(y,R)}v(x)\Big)\mid\Phi_1(b(o,R))>0\Big]\\
&\overset{(a)}{=}\mathbb{E}_{\Phi_1}\Big[\prod_{y\in\Phi_1}\mathbb{E}_{\Phi_2}\Big(\prod_{x\in\Phi_2\cap b(y,R)}v(x)\Big)\mid\|y_0\|<R\Big]\\
&=\mathbb{E}_{\Phi_1}\Big[e^{-\lambda_{\rm I}V(R,y_0)}\prod_{y\in\Phi_1\setminus\{y_0\}}e^{-\lambda_{\rm I}V(R,y)}\mid\|y_0\|<R\Big]\\
&\overset{(b)}{=}\int_0^{2\pi}\int_0^R\frac{\tilde{f}(t)}{2\pi}e^{-\lambda_{\rm I}V(R,y_0)}\big|_{y_0=(t\cos\psi,t\sin\psi)}\\
&\quad\times\exp\Big(-\beta\int_{b^c(o,t)}1-e^{-\lambda_{\rm I}V(R,y)}\mathrm{d}y\Big)\mathrm{d}t\mathrm{d}\psi\\
&=\int_{b(o,R)}\frac{\beta e^{-\beta\pi\|x\|^2-\lambda_{\rm I}V(R,x)}}{P_{\rm p}(R)}\\
&\quad\times\exp\Big(-\beta\int_{b^c(o,\|x\|)}1-e^{-\lambda_{\rm I}V(R,y)}\mathrm{d}y\Big)\mathrm{d}x, \quad (31)
\end{aligned}$$

where step (a) follows from Slivnyak's theorem applied to Φ_2 and $b^c(o,t)=\mathbb{R}^2\setminus b(o,t)$ and step (b) follows that $\tilde{f}(t)=\frac{2\pi\beta t}{P_{\rm p}(R)}e^{-\beta\pi t^2}$ is the conditional pdf of $\|y_0\|$ conditioning on $\|y_0\|<R$. Since $\Phi_2\cap b(y_0,R)\subset\Phi_2\cap\Xi$, we have

$$\begin{aligned}
\mathcal{G}^![v]&<\mathbb{E}^{!o}\Big(\prod_{x\in\Phi_2\cap b(y_0,R)}v(x)\mid\Phi_1(b(o,R))>0\Big)\\
&=\mathbb{E}_{y_0}\Big[\mathbb{E}_{\Phi_2}\Big(\prod_{x\in\Phi_2\cap b(y_0,R)}v(x)\Big)\mid\|y_0\|<R\Big]\\
&=\mathbb{E}_{y_0}\Big[e^{-\lambda_{\rm I}V(R,y_0)}\mid\|y_0\|<R\Big]\\
&=\int_0^\infty\int_0^{2\pi}\frac{\tilde{f}(t)}{2\pi}e^{-\lambda_{\rm I}V(R,y_0)}\big|_{y_0=t(\cos\psi,\sin\psi)}\,\mathrm{d}t\mathrm{d}\psi\\
&=\int_{b(o,R)}\frac{\beta e^{-\beta\pi\|y\|^2-\lambda_{\rm I}V(R,y)}}{P_{\rm p}(R)}\mathrm{d}y. \quad (32)
\end{aligned}$$

∎

Appendix C
Proof of Corollary 1

Proof: To capture the effect from the interfering nodes outside the closest ball $b(y_0,R)$, we adopt a PPP denoted by $\Phi_{\rm out}$ with density $\lambda_{\rm p}$ to approximate the spatial distribution of these nodes. Letting $\Psi_{\rm p}=\Phi_{\rm p}^o\cap b(y_0,R)$ we have

$$\begin{aligned}
\mathcal{L}_{I^!}(s)&\approx\mathbb{E}^{!o}\Big[\prod_{x\in\Psi_{\rm p}}\frac{1}{1+s\ell(x)}\prod_{x\in\Phi_{\rm out}}\frac{1}{1+s\ell(x)}\Big]\\
&=\frac{2\pi\lambda_{\rm f}}{P_{\rm p}(R)}\int_0^R e^{-\lambda_{\rm f}\pi v^2}ve^{-\lambda_{\rm d}\int_{b(y_0,R)}1-\frac{1}{1+s\ell(x)}\mathrm{d}x}\\
&\quad\times\exp\Big(-\lambda_{\rm p}\int_{b^c(y_0,R)}1-\frac{1}{1+s\ell(x)}\mathrm{d}x\Big)\mathrm{d}v\\
&\overset{(a)}{\approx}\frac{2\pi\lambda_{\rm f}}{P_{\rm p}(R)}\int_0^R e^{-\lambda_{\rm f}\pi v^2}ve^{-\lambda_{\rm d}\int_{b(y_0,R)}\frac{1}{1+s^{-1}\ell^{-1}(x)}\mathrm{d}x}\\
&\quad\times\exp\Big(-\lambda_{\rm p}\int_{b^c(o,v+R)}\frac{1}{1+s^{-1}\ell^{-1}(x)}\mathrm{d}x\Big)\mathrm{d}v, \quad (33)
\end{aligned}$$

where step (a) follows from the fact $b^c(o,v+R)\subset b^c(y_0,R)$. The final result is obtained by using polar coordinates. ∎

References

[1] M. Haenggi, *Stochastic geometry for wireless networks*. Cambridge University Press, 2012.

[2] K. Huang and V. K. N. Lau, "Enabling wireless power transfer in cellular networks: Architecture, modeling and deployment," *IEEE Transactions on Wireless Communications*, vol. 13, no. 2, pp. 902–912, Feb. 2014.

[3] A. H. Sakr and E. Hossain, "Analysis of K-tier uplink cellular networks with ambient RF energy harvesting," *IEEE Journal on Selected Areas in Communications*, vol. 33, no. 10, pp. 2226–2238, Oct. 2015.

[4] I. Krikidis, "Simultaneous information and energy transfer in large-scale networks with/without relaying," *IEEE Transactions on Communications*, vol. 62, no. 3, pp. 900–912, Mar. 2014.

[5] S. Lee, R. Zhang, and K. Huang, "Opportunistic wireless energy harvesting in cognitive radio networks," *IEEE Transactions on Wireless Communications*, vol. 12, no. 9, pp. 4788–4799, Sept. 2013.

[6] N. Deng and M. Haenggi, "The energy and rate meta distributions in wirelessly powered D2D networks," *IEEE Journal on Selected Areas in Communications*, vol. 37, no. 2, pp. 269–282, Feb 2019.

[7] X. Zhou, J. Guo, S. Durrani, and M. Di Renzo, "Power beacon-assisted millimeter wave ad hoc networks," *IEEE Transactions on Communications*, vol. 66, no. 2, pp. 830–844, Feb 2018.

[8] N. Deng and M. Haenggi, "Energy correlation in wirelessly powered networks," in *IEEE International Conference on Communications (ICC'19)*, Shanghai, China, May 2019.

[9] F. Fleischer, C. Gloaguen, H. Schmidt, V. Schmidt, and F. Schweiggert, "Simulation algorithm of typical modulated Poisson-Voronoi cells and application to telecommunication network modelling," *Japan Journal of Industrial & Applied Mathematics*, vol. 25, no. 3, pp. 305–330, 2008.

[10] R. K. Ganti and M. Haenggi, "Regularity in sensor networks," in *2006 International Zurich Seminar on Communications*. IEEE, 2006, pp. 186–189.

[11] C. Lee and M. Haenggi, "Interference and outage in Poisson cognitive networks," *IEEE Transactions on Wireless Communications*, vol. 11, no. 4, pp. 1392–1401, April 2012.

[12] J. Gil-Pelaez, "Note on the inversion theorem," *Biometrika*, vol. 38, pp. 481–482, Dec. 1951.